Adsorption (2007) 13: 139–147
DOI 10.1007/s10450-007-9015-7

The effect of burn-off on the adsorption of N_2 and Ar on a natural graphite

Kazuhisa Miura · Hiroshi Yanazawa · Kazuyuki Nakai

Received: 4 July 2005 / Revised: 13 January 2007 / Accepted: 5 July 2007 / Published online: 2 September 2007
© Springer Science+Business Media, LLC 2007

Abstract Adsorption-desorption isotherms of N_2 and Ar were measured at 77 K using samples of graphite that were partially burned off at 600 °C in O_2 gas saturated with water vapor at 25 °C. The amounts of adsorbed N_2 and Ar dropped drastically as the degree of burn-off increased. The isotherms all showed a steep rise, or step, in the amounts of adsorbed N_2 and Ar at a relative pressure of around 0.4. Moreover, the hysteresis was much narrower after burn-off than before. These anomalies can be explained by the presence of functional groups on the graphite that produce H_2O and CO_2 upon decomposition and in terms of pores on the surface of the graphite.

Keywords Natural graphite · Adsorption · Burn-off · Porosity

1 Introduction

Various oxygen-containing functional groups (carboxyl, lactone, hydroxyl, carbonyl) are present around the periphery of hexagonal condensed-carbon rings of crystallites (Boehm and Diehl 1962), and play an important role in gas adsorption phenomena (Griffiths et al. 1964; Walker Jr. and Janov 1968; Barton et al. 1973; Møller and Fort 1975; Dubinin and Serpinsky 1981; Barton et al. 1984; Miura and Morimoto 1986; Kwon et al. 2002; Slasli et al. 2004). As might be expected, the numbers and types of groups affect the adsorptivity of gases on a material, as has been reported in many studies on carbonaceous materials subjected to various treatments, such as burn-off in O_2 or air (Griffiths et al. 1964; Walker Jr. and Janov 1968; Miura and Morimoto 1986), liquid-phase treatment using various concentrations of HNO_3 (Barton et al. 1984), and O_2 plasma treatment (Kwon et al. 2002). In those studies, polar adsorbates, such as water vapor, exhibited a higher adsorptivity after oxidation of a surface than before (Walker Jr. and Janov 1968; Barton et al. 1984); N_2 and Ar have also been used as adsorbates in place of water (Griffiths et al. 1964; Møller and Fort 1975; Kwon et al. 2002).

In this study, adsorption-desorption isotherms of N_2 and Ar were measured at 77 K using samples of graphite that were partially burned off at 600 °C in moist O_2 gas. The amount of adsorbed gases was much smaller after oxidation than before. Every isotherm had a steep rise, or step, in the amount adsorbed at a relative pressure (X) of around 0.4 (Miura and Yanazawa 2003). Moreover, the hysteresis became narrower as the degree of burn-off increased. This paper reports on an investigation of these phenomena as they relate to the numbers of oxygen-containing functional groups and the width of slit-shaped pores.

2 Experimental

The starting material for the burn-off treatment is Sri Lankan natural-graphite powder that is sold as Graphite ACP by Nippon Kokuen Co. We call this starting material G25 (Mo-

K. Miura (✉)
Department of General Education, Tsuyama National College of Technology, 624-1 Numa, Tsuyama 708-8509, Japan
e-mail: miura@tsuyama-ct.ac.jp

H. Yanazawa
MEMS-CORE Co., Ltd., 2-14-9 Tateno, Higashiyamato, Tokyo 207-0021, Japan

K. Nakai
Technical Department, Bel Japan, Inc., 1-5-6 Ebie, Fukushima-ku, Osaka 553, Japan

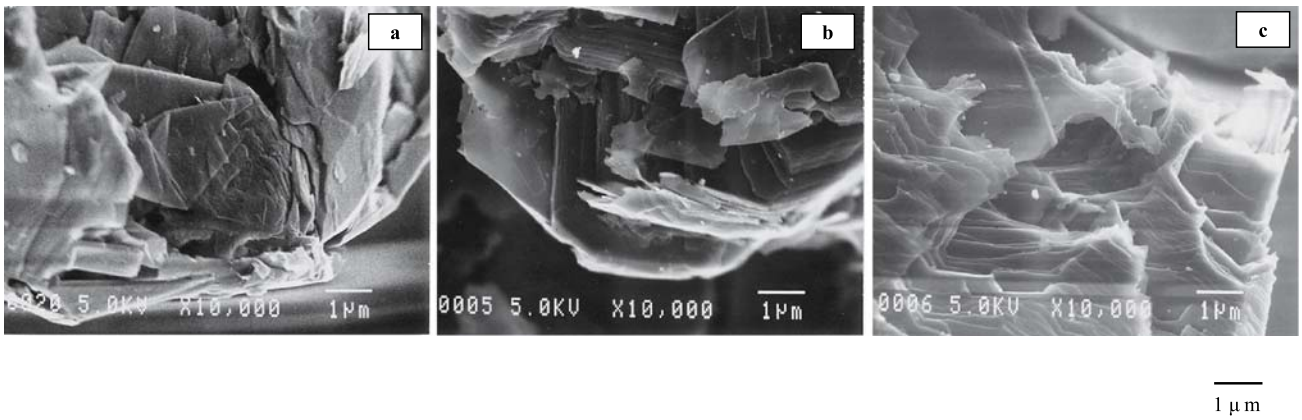

Fig. 1 SEM images of samples of (**a**) G25, (**b**) OGA, and (**c**) OGB

rimoto and Miura 1985). It is 99.5% pure and contains 0.5% ash. The particles are 1–30 μm in diameter.

Samples of G25 in a quartz tube were partially burned off at 600 °C in a flow of O_2 and H_2O gases, as described in a previous study (Miura and Morimoto 1986). This yielded two kinds of samples: OGA, for which the weight loss was 18%; and OGB, for which it was 51%. For reference, a third type of sample, labeled G500, was prepared by pyrolyzing G25 at 500 °C in an N_2 flow.

Adsorption-desorption isotherms were measured at 77 K with the BEL-SORP automatic adsorption-measuring apparatus made by Bel Japan, Inc. The BET specific surface area of each sample was calculated from the measured N_2 adsorption isotherm, assuming a value of 0.162 nm^2 for the cross-sectional area of an N_2 molecule at 77 K.

Samples were heated from room temperature to 1000 °C, and the gas expelled was analyzed quantitatively by gas chromatography and also by alternately using two traps, one at −196 °C and the other at −78 °C (Morimoto and Miura 1985). From among the various gases expelled, we focused on H_2O and CO_2 for the reasons given below.

SEM observations were made with a JEOL–JSM890 electron microscope at an operating voltage of 5 kV.

3 Results and discussion

3.1 SEM observations

The SEM images of OGA, OGB, and G25 in Fig. 1 show that burn-off eroded the prism plane; that is, its morphology becomes more clear-cut, or geometric, as the degree of burn-off increases. In contrast, the stacking layer on G25 is so jumbled that the orientation of the prism plane appears complicated, which means that the surface is morphologically heterogeneous. It can thus be inferred that erosion removes the complication in the orientation of the prism plane. In addition, semicircular shapes can be seen on the prism planes of both OGA and OGB. The same kind of shape was also observed in a previous study (Miura and Morimoto 1986); and Kwon et al. reported a similar morphology on the surface of HOPG oxidized with O_2 plasma (Kwon et al. 2002).

3.2 H_2O- or CO_2-producing surface functional groups

Figures 2 and 3 show how the amounts of H_2O and CO_2, respectively, expelled from graphite samples depend on pyrolysis temperature. Functional groups on the surface of carbonaceous materials thermally decompose into various gases consisting of carbon, hydrogen, and/or oxygen, which come mainly from functional groups bonded to the carbon atoms constituting the skeleton of basal planes (Coltharp and Hackerman 1968). When carboxyl, lactone, and hydroxyl groups thermally decompose, they produce H_2O and CO_2 (Miura and Morimoto 1988). These groups are comparatively large and project out from the hexagonal carbon skeleton; and they seem to influence the formation of pores in the graphite (Miura and Yanazawa 2003). This fact made us turn our attention to the amounts of these gases that are expelled.

In both Fig. 2 and Fig. 3, the curves for OGA and OGB are completely different from the one for G25 in that the number of H_2O- and CO_2-producing groups that decompose below 600 °C (burn-off temperature) is markedly lower, while the number of such groups that decompose above 600 °C is much greater. This difference appears as a single peak above 600 °C for CO_2 and a small but distinct peak around 700 °C for H_2O. This suggests that the environment of the CO_2- and H_2O-producing groups on OGA and OGB is different from that on G25, owing to the high-temperature burn-off, and more importantly, that one kind of CO_2-producing group with almost the same thermal stability on both burn-off samples is prevalent on the surface of those samples. This indicates that, from the standpoint of energy, the surfaces are rather homogeneous.

3.3 Adsorption-desorption isotherms of N_2 and Ar

In this investigation, we used Ar as an adsorbate, in addition to N_2. The reason is due to the fact that Ar is often used in the investigations (Møller and Fort 1975; Gregg and Sing 1982; Banáres-Muńoz et al. 1987; Ismail 1992; Miura and Yanazawa 2003; Do and Do 2005) similar to this study, which makes us compare easily the present data to those concerning artificial graphite samples.

The adsorption-desorption isotherms of N_2 (Fig. 4) and Ar (Fig. 5) for each sample taken at 77 K show a small but distinct step at a relative pressure (X) of around 0.4. This step can be seen more clearly in the inset of each figure. The step found here can be considered to be the same as reported in the previous work (Miura and Yanazawa 2003).

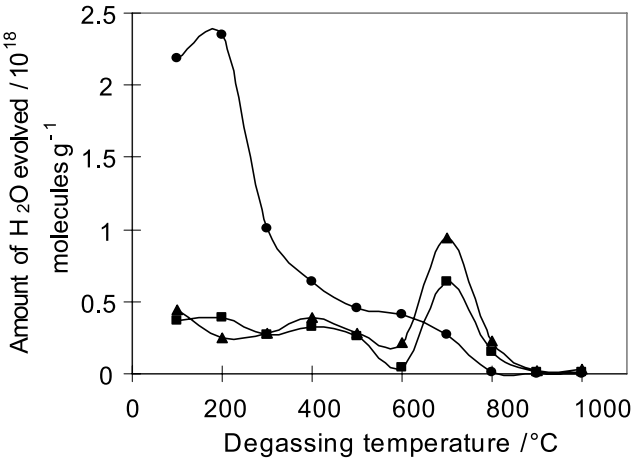

Fig. 2 Amount of H_2O evolved at intervals of 100 °C from samples subjected to heating: ●: G25, ■: OGA, ▲: OGB

Figure 6 compares adsorption-desorption isotherms of N_2 for samples G500 and G25. As mentioned with regard to Figs. 2 and 3, pyrolysis at 500 °C undoubtedly removes any functional groups that decompose below this temperature. So, the surface of G500 was expected to be in a different condition from that of G25. However, the isotherms of the two samples have a similar shape.

Table 1 shows the BET monolayer capacity (V_m), the specific surface area, and the C-value obtained by applying the BET method to the adsorption isotherms (Figs. 4, 5 and 6). These data show that burn-off drastically reduces the specific surface area of graphite. Besides this, every BET plot of N_2 adsorption data was found to have a discontinuity and to consist of two linear portions in the ranges $0 \leq X \leq 0.17$ and $0.17 \leq X \leq 0.35$. We used the line in the lower pressure region to calculate the specific surface area, based on a previous study (Miura and Yanazawa 2003) and a report by Møller and Fort (1975). It is interesting to note that the degree of discontinuity (i.e., the difference between the slopes of the two linear sections) becomes more pronounced as the degree of burn-off increases, although there is no discontinuity in a BET plot of the Ar adsorption data.

Tables 2 and 3 are the tabulated adsorption data for N_2 and Ar, respectively. Here, θ is the surface coverage of each gas, being equal to V/V_m.

Figures 7 and 8 are the normalized adsorption isotherms of N_2 and Ar, respectively, where the amount adsorbed is ex-

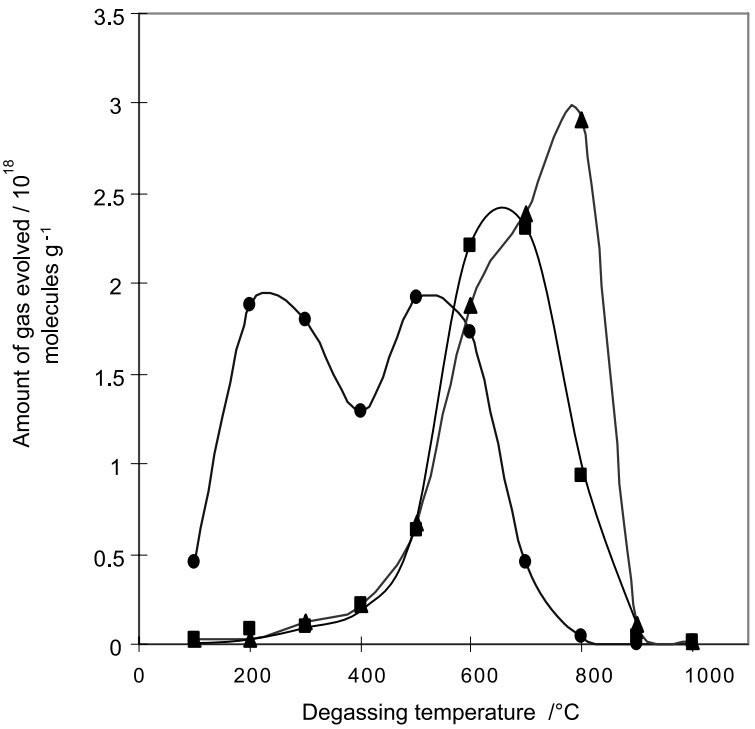

Fig. 3 Amount of CO_2 evolved at intervals of 100 °C from samples subjected to heating: ●: G25, ■: OGA, ▲: OGB

Table 1 Adsorption capacity (V_m), C-value, and specific surface area

	Nitrogen adsorption			Argon adsorption		
	V_m (cm^3/g)	C-value	Surface area (m^2/g)	V_m (cm^3/g)	C-value	Surface area (m^2/g)[a]
G25	2.83	443	12.30	3.16	352	11.70
OGA	1.30	849	5.66	1.42	653	5.27
OGB	0.90	2242	3.94	1.06	443	3.91
G500	3.07	586	13.40	3.40	352	12.60

[a]The Ar surface area was estimated assuming the cross-sectional area of an Ar molecule at 77 K to be 0.138 nm^2

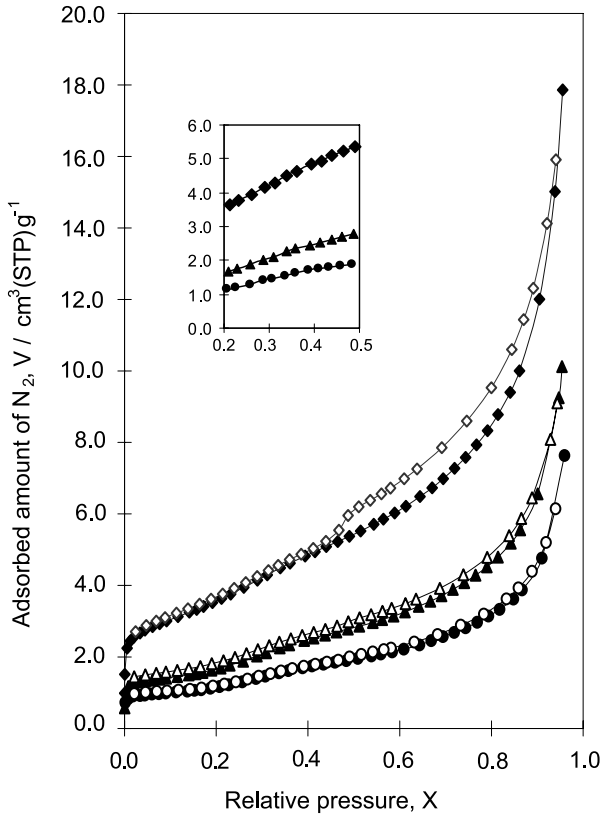

Fig. 4 Adsorption-desorption isotherms of N_2 on graphite samples at 77 K. *Filled marks*: adsorption; *open marks*: desorption. ◆, ◇: G25, ▲, △: OGA, ●, ○: OGB. The *inset* is an expanded view of the region around the JE step

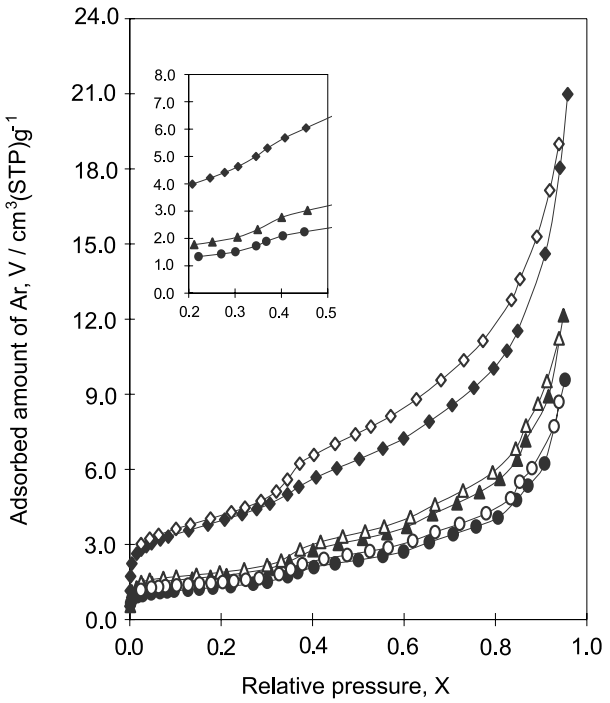

Fig. 5 Adsorption-desorption isotherms of Ar on graphite samples at 77 K. *Filled marks*: adsorption; *open marks*: desorption. ◆, ◇: G25, ▲, △: OGA, ●, ○: OGB. The *inset* is an expanded view of the region around the JE step

pressed in terms of surface coverage, $\theta(= V/V_m)$. These figures demonstrate impressive contrast between the isotherm for G25 and those for both OGA and OGB, i.e., the θ value increases suddenly at the relative pressure corresponding to appearance of the step in the case of OGA or OGB. And besides, the two normalized isotherms of N_2 on both samples almost coincide, which indicates that the N_2 adsorption proceeds in the same manner, compared to G25. The same feature is also found in the case of Ar adsorption.

Figures 9 and 10 are the N_2 and Ar adsorption isotherm, respectively, with both axes drawn in logarithmic scale according to the literature (Kruk et al. 1999; Gardner et al. 2001; Do and Do 2005). The adsorbed amounts of both gases at $X \approx 0$ have betrayed their real nature, as found in those figures: they are thus divided into different points on the abscissa.

Gardner et al. measured adsorption isotherms of Ar on carbon blacks very precisely before and after graphitization (Gardner et al. 2001), and Kruk et al. obtained adsorption isotherms of N_2 on graphitized carbon blacks with a higher precision (Kruk et al. 1999). In both minute investigations, the adsorption energy was also calculated. Actually, our data are not so precise as theirs. However, the burn-off

Table 2 N_2 adsorption data for each graphite sample at 77 K

G25			OGA			OGB		
X	V/cm^3 (STP)· g^{-1}	θ	X	V/cm^3 (STP)· g^{-1}	θ	X	V/cm^3 (STP)· g^{-1}	θ
3.62×10^{-4}	0.9880	0.3491	3.18×10^{-4}	0.5751	0.4424	1.50×10^{-3}	0.7262	0.8069
6.03×10^{-4}	1.5154	0.5355	8.44×10^{-3}	1.1729	0.9022	8.09×10^{-3}	0.8322	0.9247
5.55×10^{-3}	2.2464	0.7938	1.89×10^{-2}	1.2575	0.9673	1.84×10^{-2}	0.9052	1.0058
1.22×10^{-2}	2.4440	0.8636	3.45×10^{-2}	1.2970	0.9977	3.39×10^{-2}	0.9224	1.0249
1.92×10^{-2}	2.5425	0.8984	4.48×10^{-2}	1.3195	1.0150	4.40×10^{-2}	0.9326	1.0362
3.36×10^{-2}	2.6704	0.9436	6.10×10^{-2}	1.3534	1.0411	5.97×10^{-2}	0.9608	1.0676
4.46×10^{-2}	2.7505	0.9719	7.62×10^{-2}	1.3771	1.0593	7.48×10^{-2}	0.9713	1.0792
6.11×10^{-2}	2.8494	1.0069	9.10×10^{-2}	1.4089	1.0838	8.98×10^{-2}	0.9919	1.1021
7.65×10^{-2}	2.9297	1.0352	0.1151	1.4527	1.1175	0.1124	1.0187	1.1319
9.16×10^{-2}	3.0051	1.0619	0.1401	1.5008	1.1545	0.1373	1.0426	1.1584
0.1166	3.1288	1.1056	0.1552	1.5302	1.1771	0.1525	1.0658	1.1842
0.1416	3.2518	1.1490	0.1703	1.5640	1.2031	0.1674	1.0824	1.2027
0.1575	3.3304	1.1768	0.1898	1.6327	1.2559	0.1873	1.1253	1.2503
0.1724	3.4102	1.2050	0.2098	1.6927	1.3021	0.2072	1.1702	1.3002
0.1919	3.5225	1.2447	0.2296	1.7706	1.3620	0.2273	1.2207	1.3563
0.2117	3.6377	1.2854	0.2589	1.8838	1.4491	0.2569	1.3030	1.4478
0.2317	3.7586	1.3281	0.2887	2.0254	1.5580	0.2867	1.3975	1.5528
0.2601	3.9457	1.3942	0.3091	2.1184	1.6295	0.3070	1.4626	1.6251
0.2899	4.1469	1.4653	0.3386	2.2538	1.7337	0.3368	1.5556	1.7284
0.3113	4.2970	1.5184	0.3593	2.3391	1.7993	0.3574	1.6165	1.7961
0.3396	4.4892	1.5863	0.3917	2.4621	1.8939	0.3882	1.6930	1.8811
0.3608	4.6239	1.6339	0.4123	2.5325	1.9481	0.4088	1.7454	1.9393
0.3937	4.8238	1.7045	0.4373	2.6132	2.0102	0.4337	1.7990	1.9989
0.4154	4.9445	1.7472	0.4621	2.7014	2.0780	0.4589	1.8548	2.0609
0.4398	5.0869	1.7975	0.4873	2.7813	2.1395	0.4838	1.8964	2.1071
0.4650	5.2277	1.8472	0.5121	2.8635	2.2027	0.5087	1.9584	2.1760
0.4902	5.3756	1.8995	0.5415	2.9631	2.2793	0.5384	2.0249	2.2499
0.5147	5.5232	1.9517	0.5620	3.0482	2.3448	0.5588	2.0812	2.3124
0.5434	5.7119	2.0183	0.5867	3.1431	2.4176	0.5836	2.1404	2.3782
0.5645	5.8553	2.0690	0.6115	3.2592	2.5071	0.6089	2.2179	2.4643
0.5890	6.0276	2.1299	0.6413	3.4144	2.6265	0.6432	2.3344	2.5938
0.6136	6.2164	2.1966	0.6668	3.5601	2.7385	0.6688	2.4559	2.7288
0.6441	6.4859	2.2918	0.6913	3.7152	2.8578	0.6943	2.5676	2.8529
0.6706	6.7300	2.3781	0.7161	3.8901	2.9924	0.7188	2.6850	2.9833
0.6948	6.9859	2.4685	0.7408	4.0774	3.1365	0.7435	2.8140	3.1267
0.7195	7.2768	2.5713	0.7654	4.2899	3.2999	0.7688	2.9692	3.2991
0.7437	7.5814	2.6789	0.7899	4.5215	3.4781	0.7935	3.1435	3.4928
0.7674	7.9316	2.8027	0.8143	4.7913	3.6856	0.8177	3.3297	3.6997
0.7914	8.3288	2.9430	0.8423	5.1818	3.9860	0.8478	3.6180	4.0200
0.8142	8.7784	3.1019	0.8627	5.5536	4.2720	0.8666	3.8753	4.3059
0.8408	9.4006	3.3218	0.9009	6.5602	5.0463	0.9099	4.7647	5.2941
0.8611	10.003	3.5346	0.9468	9.2519	7.1168	0.9592	7.6331	8.4812
0.9045	12.006	4.2424	0.9537	10.121	7.7854			
0.9384	15.017	5.3064						
0.9551	17.859	6.3106						

Table 3 Ar adsorption data for each graphite sample at 77 K

G25			OGA			OGB		
X	V/cm^3 (STP)·g^{-1}	θ	X	V/cm^3 (STP)·g^{-1}	θ	X	V/cm^3 (STP)·g^{-1}	θ
2.98×10^{-4}	0.5361	0.1697	1.19×10^{-3}	0.5450	0.3838	2.07×10^{-3}	0.6526	0.6157
8.94×10^{-4}	1.1452	0.3624	4.31×10^{-3}	1.1235	0.7912	7.56×10^{-3}	0.8584	0.8098
1.79×10^{-3}	1.7237	0.5455	1.50×10^{-2}	1.2831	0.9036	1.71×10^{-2}	0.9288	0.8762
4.63×10^{-3}	2.2388	0.7085	2.92×10^{-2}	1.3612	0.9586	2.81×10^{-2}	0.9708	0.9158
1.53×10^{-2}	2.6341	0.8336	4.85×10^{-2}	1.4571	1.0261	4.70×10^{-2}	1.0471	0.9878
2.49×10^{-2}	2.7932	0.8839	7.10×10^{-2}	1.5123	1.0650	6.65×10^{-2}	1.0949	1.0329
3.64×10^{-2}	2.9302	0.9273	0.1009	1.5752	1.1093	8.21×10^{-2}	1.1244	1.0608
4.78×10^{-2}	3.0468	0.9642	0.1369	1.6367	1.1526	9.73×10^{-2}	1.1532	1.0879
6.68×10^{-2}	3.1992	1.0124	0.1766	1.7052	1.2008	0.1274	1.1923	1.1248
8.44×10^{-2}	3.3134	1.0485	0.2117	1.7745	1.2496	0.1522	1.2328	1.1630
0.1291	3.5658	1.1284	0.2511	1.8685	1.3158	0.1821	1.2750	1.2028
0.1711	3.7902	1.1994	0.3053	2.0453	1.4404	0.2212	1.3369	1.2612
0.2079	3.9899	1.2626	0.3489	2.3261	1.6381	0.2702	1.4319	1.3508
0.2460	4.2141	1.3336	0.4008	2.7684	1.9496	0.3010	1.5104	1.4249
0.2776	4.4141	1.3969	0.4565	3.0248	2.1301	0.3456	1.7292	1.6313
0.3064	4.6290	1.4649	0.5097	3.2282	2.2734	0.3675	1.8922	1.7851
0.3452	5.0009	1.5826	0.5627	3.4524	2.4313	0.4029	2.0931	1.9746
0.3699	5.3021	1.6779	0.6059	3.7043	2.6087	0.4495	2.2415	2.1146
0.4076	5.6789	1.7971	0.6624	4.2089	2.9640	0.5004	2.3767	2.2422
0.4532	6.0410	1.9117	0.7159	4.6465	3.2722	0.5538	2.5404	2.3966
0.5023	6.4140	2.0297	0.7651	5.0907	3.5850	0.5990	2.7183	2.5644
0.5540	6.8251	2.1598	0.8100	5.6189	3.9570	0.6554	3.0923	2.9173
0.5990	7.2312	2.2884	0.8480	6.3881	4.4987	0.7076	3.4078	3.2149
0.6551	7.9057	2.5018	0.8664	7.1563	5.0396	0.7579	3.7164	3.5060
0.7053	8.5676	2.7113	0.9163	8.9210	6.2824	0.8059	4.0776	3.8468
0.7529	9.2560	2.9291	0.9487	12.151	8.5570	0.8462	4.7716	4.5015
0.7963	10.032	3.1747				0.8712	5.3473	5.0446
0.8253	10.736	3.3975				0.9075	6.2346	5.8817
0.8487	11.531	3.6491				0.9524	9.5768	9.0347
0.9088	14.603	4.6212						
0.9412	18.041	5.7092						
0.9582	20.980	6.6392						

treatment clearly gives rise to a few remarkable changes in the adsorption-desorption isotherms of both gases, as listed below.

These figures and table reveal that, as the degree of burn-off increases,

(1) the amount of adsorbed gases drops drastically;
(2) the step becomes more prominent, and it is larger for Ar than for N_2;
(3) the hysteresis becomes less pronounced.

As shown in Figs. 9 and 10, the amount adsorbed in the very early stage drops. This fact suggests that burn-off treatment demolishes micropores on OGA and OGB. And, clearly the amount adsorbed over the whole range of equilibrium pressure decreases in every case. These are related to (1) above.

Griffiths et al. examined the effect of burn-off on the heterogeneity of the surface of various types of graphitized carbon, and found that the N_2 specific surface area increased with increasing degree of burn-off (Griffiths et al. 1964). Interestingly, that is the opposite of what we found. The difference may be attributable either to the difference between the oxidizing gases used for burn-off (spectroscopically pure O_2 in their case vs. moist O_2 in ours) or to the difference between the kinds of carbonaceous material used (graphitized carbon black for them vs. natural graphite for us).

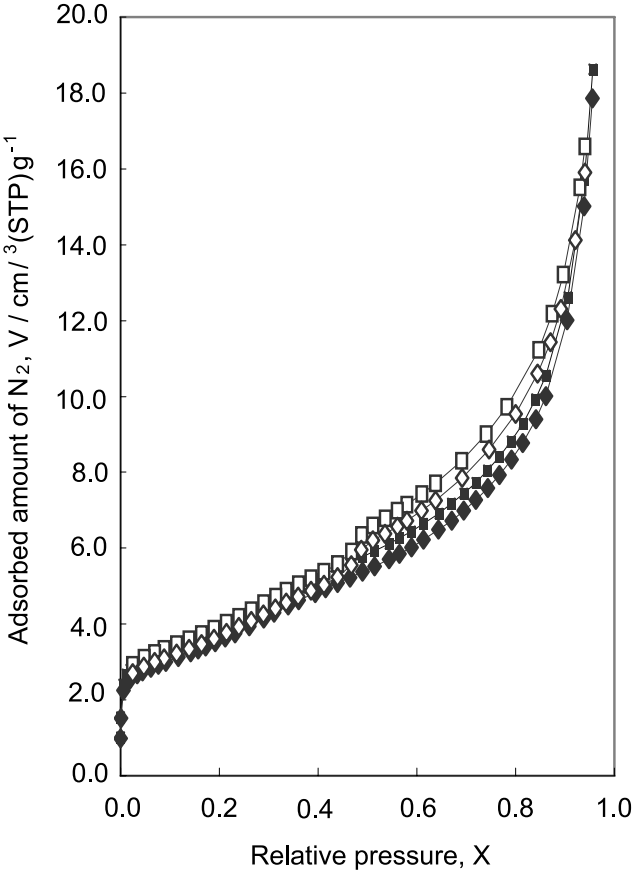

Fig. 6 Adsorption-desorption isotherms of N_2 on graphite samples at 77 K. *Filled marks*: adsorption; *open marks*: desorption. ◆, ◇: G25, ■, □: G500

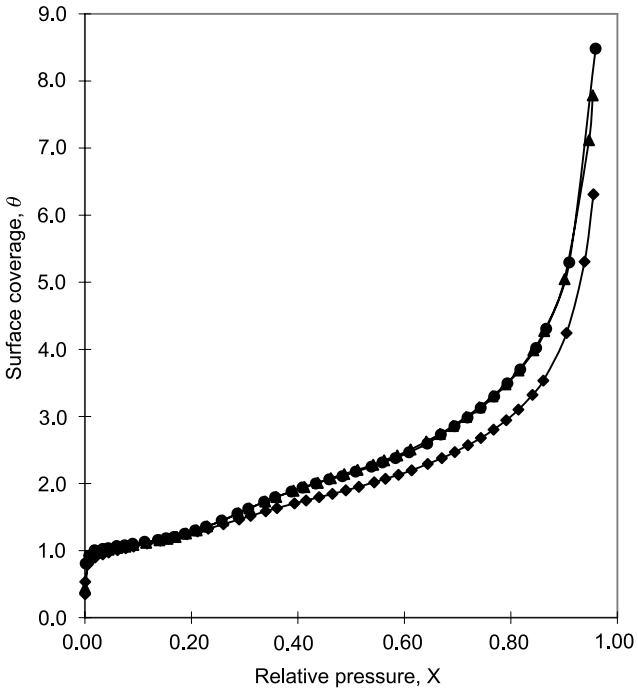

Fig. 7 Normalized adsorption isotherms of N_2 on graphite samples at 77 K. ◆: G25, ▲: OGA, ●: OGB

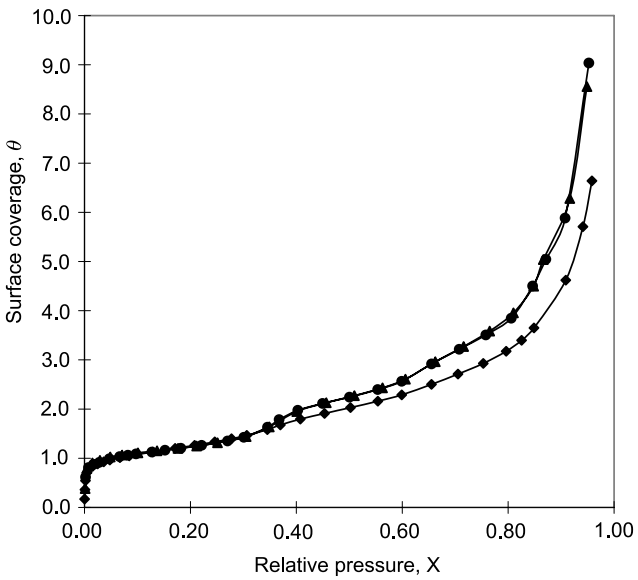

Fig. 8 Normalized adsorption isotherms of Ar on graphite samples at 77 K. ◆: G25, ▲: OGA, ●: OGB

Regarding (2) above, the step can be thought of as reflecting the process by which a second adsorption layer forms. Here, the procedure in a previous study (Miura and Yanazawa 2003) is used to estimate the amount adsorbed at the end of the step for each adsorption isotherm. The results are shown in Table 4, where the amount adsorbed at the end of the step is given in terms of V_m. Assuming that all the pores are accessible to gas molecules, the amount adsorbed at the end of the step should be approximately $2V_m$. It can be inferred from this that the surfaces of both OGA and OGB are completely accessible to N_2 molecules and Ar atoms, while there are many pores on the surface of G25 that are inaccessible to both. This means that OGA and OGB probably have flatter surfaces than G25 does, because the moist O_2 gas burned off the walls of the pores (hexagonal condensed-carbon rings) on G25 along with their functional groups, thus making the pores shallower. The affected functional groups probably have a different alignment with respect to the peripheries of nearby hexagonal carbon rings than they had prior to burn-off.

As stated above, only (newly created) functional groups with almost the same heat resistance are prevalent on both OGA and OGB. Burn-off, therefore, enhances the homogeneity of the graphite surface to some extent, thereby making the step more pronounced for both samples.

3.4 Hysteresis

The hysteresis seems to result from the presence of pores (Miura and Yanazawa 2003). Figure 11 shows the t-plots

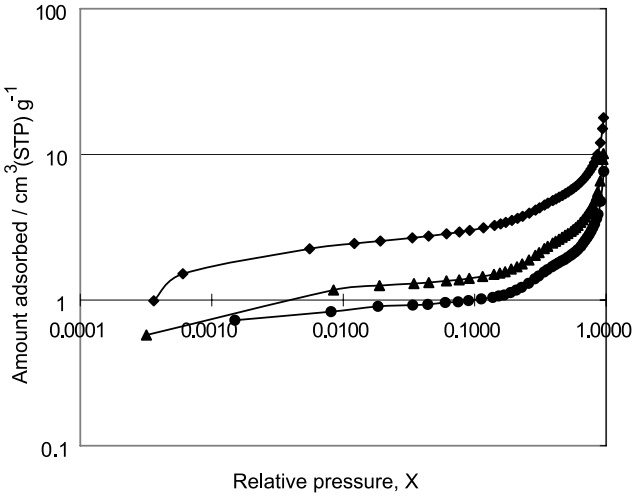

Fig. 9 Adsorption isotherms of N_2 on graphite samples at 77 K, drawn in logarithmic scale. ◆: G25, ▲: OGA, ●: OGB

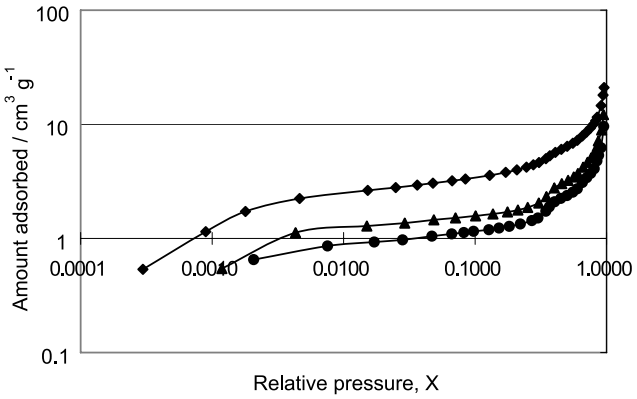

Fig. 10 Adsorption isotherms of Ar on graphite samples at 77 K, drawn in logarithmic scale. ◆: G25, ▲: OGA, ●: OGB

Table 4 Amount of gas adsorbed at end of the step appeared around X = 0.4

	N_2	Ar
G25	$1.74V_m$	$1.84V_m$
OGA	$2.03V_m$	$2.08V_m$
OGB	$2.03V_m$	$2.05V_m$
G500	$1.73V_m$	$1.88V_m$

calculated from the adsorption isotherms of N_2 (Figs. 4 and 6). For the t-method calculations, a master t-curve, which was proposed by Smith and Kasten (Smith and Kasten 1970), was used. In order to make the calculations more valid, the recent t-curve in ASTM Method was also checked (ASTM Method D6556-01 2002). The t-curves calculated from the master t-values in both reports (Smith and Kasten 1970; ASTM Method D6556-01 2002) coincided. Calculations of the slopes of the initial dotted lines yielded surface areas of 4.26, 5.96, 12.61, and 14.04 m^2/g for OGB,

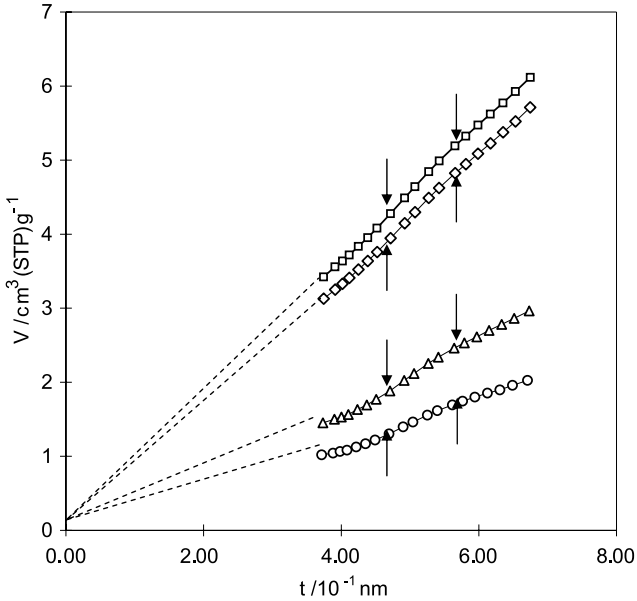

Fig. 11 t-plots of adsorption isotherms of N_2 for graphite samples: (◇) G25; (△) OGA; (○) OGB; (□) G500. *Arrows* show breaks in each line

OGA, G25, and G500, respectively. These values are close to the BET surface areas listed in Table 1, confirming the accuracy of the master t-values.

Figure 11 also reveals the following facts: (i) relatively gentle slopes of the initial lines up to t = 0.47 nm for both OGA and OGB show that these samples are rather flat compared to G25 and G500. This agrees well the fact that the difference between adsorption and desorption branches for OGA or OGB sample is not so large as for G25 or G500. (ii) Every plot can be found to slope upward at t = 0.47 nm, and downward at t = 0.57 nm: it can be conjectured that N_2 molecules are filling the slit-shaped pores with width between 0.94 nm and 1.14 nm on every sample of graphite. And moreover, the amount of N_2 filled, i.e., the difference in the vertical line between the two breakpoints, becomes smaller as the degree of burn-off is raised, which reveals that burn-off made the pores of graphite samples shallower. On the other hand, the pyrolysis in the N_2 flow did not significantly affect the size and the depth of pores, as just stated above.

Burn-off with O_2 and H_2O molecules probably breaks down the walls of pores, which are made of hexagonal condensed-carbon rings, thereby making the prism plane flatter. This change occurred in the prism plane causes the decrease in the specific surface area. This fact is consistent with the calculation results in Table 2.

The H_2O- and CO_2-producing groups that decompose at temperatures below 500 °C are purged from the surface of G500; and based on Figs. 2 and 3, most of the H_2O-producing groups have disappeared, and only the CO_2-producing groups with an evolution peak around 600 °C are

present. One would naturally expect that pores with different sizes from those of G25 prevail on G500. However, the t-plots for the two samples are quite similar, which strongly suggests that the functional groups around the periphery of hexagonal carbon rings, which project outward, do not greatly affect the depth of mesopores.

4 Conclusion

Sri Lankan graphite was subjected to burn-off in moist O_2 gas at a temperature of 600 °C; and N_2 and Ar adsorption isotherms as well as of the amount of H_2O and CO_2 expelled during pyrolysis at temperatures of up to 1000 °C were measured for treated and untreated samples. It was found that burn-off breaks down the walls of pores, thereby making the prism surface flatter. In addition, contrary to expectations, a surface subjected to burn-off becomes somewhat more homogeneous for both N_2 and Ar.

Acknowledgement The authors would like to thank Prof. Kunimitsu Morishige of the Okayama University of Science for his help with the electron microscopy experiments.

References

ASTM Method D6556-01 (Standard test method for carbon black—total and external surface area by nitrogen adsorption), http://www.astm.org/cgi-bin/SoftCart.exe/DATABASE.CART/D.htm?L+mystore+elrn1790+1006167341. (2002)

Banáres-Muńoz, M.A., Flores González, L.V., Martín Llorenta, J.M.: Adsorption isotherms of nitrogen and argon on "AGOT" grade artificial nuclear graphite at 77 K and 90 K. Carbon **25**, 603–608 (1987)

Barton, S.S., Evans, M.J.B., Harrison, B.H.: Surface studies on carbon: water adsorption on polyvinylidene chloride carbon. Carbon **45**, 542–548 (1973)

Barton, S.S., Evans, M.J.B., Holland, J., Koresh, J.E.: Water and cyclohexane vapour adsorption on oxidized porous carbon. Carbon **22**, 265–272 (1984)

Boehm, H.P., Diehl, E.: Untersuchung an sauren Oberflächenoxide des Kohlenstoffs. Z. Elektrochem. **66**, 642–647 (1962)

Coltharp, M.T., Hackerman, N.: The surface of a carbon with sorbed oxygen on pyrolysis. J. Phys. Chem. **72**, 1171–1177 (1968)

Do, D.D., Do, H.D.: Adsorption of argon on homogeneous graphitized thermal carbon black and heterogeneous carbon surface. J. Colloid Interface Sci. **287**, 452–460 (2005)

Dubinin, M.M., Serpinsky, V.V.: Isotherm equation for water vapor adsorption by microporous carbonaceous adsorbents. Carbon **19**, 402–403 (1981)

Gardner, L., Kruk, M., Jaroniec, M.: Reference data for argon adsorption on graphitized and nongraphitized carbon blacks. J. Phys. Chem. B **105**, 12516–12523 (2001)

Gregg, S.J., Sing, K.S.W.: Adsorption, surface area and porosity, 2nd edn., pp. 84–89. Academic Press, London (1982)

Griffiths, D.W.L., Thomas, W.J., Walker Jr., P.L.: Effect of oxidation on the surface heterogeneity of some graphitized carbons. Carbon **1**, 515–523 (1964)

Ismail, M.K.: Cross-sectional areas of adsorbed N_2, Ar, Kr, and O_2 on carbons and fumed silicas at liquid nitrogen temperature. Langmuir **8**, 360–365 (1992)

Kruk, M., Li, Z., Jaroniec, M.: Nitrogen adsorption study of surface properties of graphitized carbon blacks. Langmuir **15**, 1435–1441 (1999)

Kwon, S., Vidic, R., Borguet, E.: Enhancement of adsorption on graphite (HOPG) by modification of surface chemical functionality and morphology. Carbon **40**, 2351–2358 (2002)

Miura, K., Morimoto, T.: Adsorption sites for water on graphite. 3. Effect of oxidation treatment of sample. Langmuir **2**, 824–828 (1986)

Miura, K., Morimoto, T.: Adsorption sites for water on graphite. 4. Chemisorption of water on graphite at room temperature. Langmuir **4**, 1283–1288 (1988)

Miura, K., Yanazawa, H.: Anomalies in standard gas adsorption isotherms of N_2 and Ar on graphite at 77 K. Carbon **41**, 151–156 (2003)

Møller, P.J., Fort Jr., T.: Structure analysis of graphite fiber surfaces. I. Mass spectrometry and low temperature adsorption of N_2 and Ar. Colloid Polym. Sci. **253**, 98–108 (1975)

Morimoto, T., Miura, K.: Adsorption site for water on graphite. 1. Effect of high-temperature treatment of sample. Langmuir **1**, 658–662 (1985)

Slasli, A.M., Jorge, M., Stoeckli, F., Seaton, N.A.: Modelling of water adsorption by activated carbons: effects of microporous structure and oxygen content. Carbon **42**, 1947–1952 (2004)

Smith, W.R., Kasten, G.A.: Porosity studies on some oil furnace black. Rubber Chem. Technol. **43**, 960–968 (1970)

Walker Jr., P.L., Janov, J.: Hydrophilic oxygen complexes on activated graphon. J. Colloid Interface Sci. **28**, 449–458 (1968)